


2023

Halogen Bonding Interactions of Haloaromatic Endocrine Disruptors and the Potential for Inhibition of Iodothyronine Deiodinases

Craig A. Bayse
Old Dominion University, cbayse@odu.edu

Follow this and additional works at: https://digitalcommons.odu.edu/chemistry_fac_pubs

 Part of the [Endocrinology, Diabetes, and Metabolism Commons](#), [Organic Chemistry Commons](#), and the [Toxicology Commons](#)

Original Publication Citation

Bayse, C. A. (2023). Halogen bonding interactions of haloaromatic endocrine disruptors and the potential for inhibition of iodothyronine deiodinases. *ChemistrySelect* 8(24), 1-8, Article e202300781.
<https://doi.org/10.1002/slct.202300781>

This Article is brought to you for free and open access by the Chemistry & Biochemistry at ODU Digital Commons. It has been accepted for inclusion in Chemistry & Biochemistry Faculty Publications by an authorized administrator of ODU Digital Commons. For more information, please contact digitalcommons@odu.edu.

Halogen Bonding Interactions of Haloaromatic Endocrine Disruptors and the Potential for Inhibition of Iodothyronine Deiodinases

Craig A. Bayse^{*[a]}

Halogen bonding (XB) is a potential mechanism for the inhibition of the thyroid-activating/deactivating iodothyronine deiodinase family of selenoproteins through interactions with halogenated endocrine disrupting compounds (EDCs). Trends in XB interactions were examined using density functional theory for a series of polyhalogenated dibenzo-1,4-dioxins, biphenyls, and other EDCs with methylselenolate, a simple model of the Dio active site selenocysteine. The strengths of the interactions depend upon the halogen (Br > Cl), the degree

of substitution, and the position of the acceptor. In terms of donor-acceptor energies, interactions at the *meta* position are often the strongest, suggesting a link to the topology of THs, especially for outer-ring deiodination of thyroxine, which occurs at a *meta* iodine, and produces the active TH. However, relationships between XB interaction strengths and potential for Dio inhibition should be made in the context of the binding to the active sites, the topology of which are not fully characterized.

Introduction

Over a decade ago, our computational models suggested a link between halogen bonding (XB)^[1,2] and the activity of the iodothyronine deiodinase (Dio) selenoproteins that regulate concentrations of thyroid hormones (TH).^[3] The Dio family removes iodine from polyiodinated thyronines like thyroxine (T₄) to activate and deactivate thyroid signaling (Figure 1A).^[4–6] Dios are regioselective, with Type II (Dio2), removing an iodine from the outer ring of T₄ to make the active TH triiodothyronine (T₃). Type III (Dio3) only deiodinates the inner ring while Type I (Dio1) can activate either site, depending upon functionalization of the substrate. In our proposed mechanism, an initially formed XB intermediate is stabilized by the protein to convert the non-bonding interaction to a nucleophilic attack at the aromatic iodine. Subsequent experimental studies and computational models have provided strong support for this initial hypothesis.^[7–11] Additionally, hydrogen shuttle pathways to facilitate deiodination via this mechanism were identified in the crystal structure of the Dio3 monomer.^[12] Although less abundant than other chalcogens and halogens, selenium and iodine are incorporated into the TH signaling pathways due to the high nucleophilicity of selenium and the low electronegativity of iodine, both properties that contribute to strong XB.

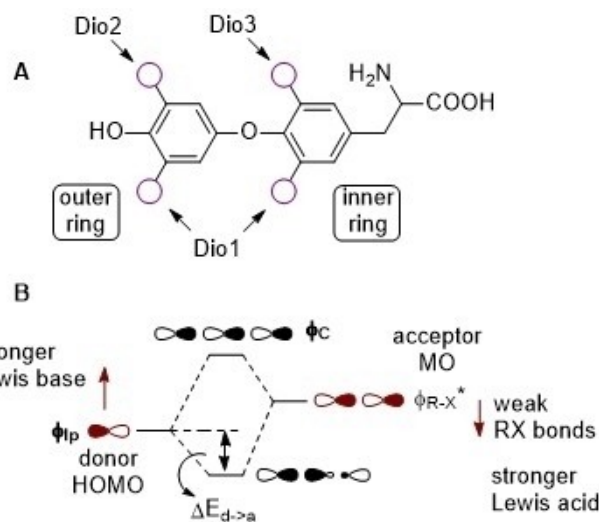


Figure 1. (A) Regioselectivity of Dio selenoproteins for inner- or outer-ring deiodination. (B) MO diagram for a donor-acceptor interaction.

A number of polyhalogenated aromatic hydrocarbons (PAHs) are listed on the Endocrine Disruption Exchange's (TEDX)^[13] catalog of potential endocrine disrupting compounds (EDCs)^[14–21] and many are known to inhibit TH signal pathways.^[17,22–27] PAHs have primarily been used as flame retardants in a variety of industrial applications.^[28,29] These persistent organic pollutants (POPs) have made their way into the food chain through chemical spills and leaching from waste including electronic waste and microplastics.^[30–33] Although the primary pathway for PAH endocrine disruption appears to be through inhibition of the aryl hydrocarbon receptor (AhR),^[34] they may also affect TH activation by Dio proteins. Halogen bonding of PAHs to the Dio active site selenocysteine (Sec) residue to prevent TH binding and activation is a potential

[a] Prof. C. A. Bayse
Department of Chemistry and Biochemistry,
Old Dominion University,
23529 Norfolk, Virginia, USA
E-mail: cbayse@odu.edu

© 2023 The Authors. ChemistrySelect published by Wiley-VCH GmbH. This is an open access article under the terms of the Creative Commons Attribution Non-Commercial NoDerivs License, which permits use and distribution in any medium, provided the original work is properly cited, the use is non-commercial and no modifications or adaptations are made.

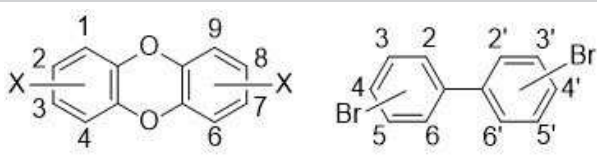
mechanism for Dio inhibition,^[35] which has been demonstrated for polychlorinated biphenyls (PCB) and polybrominated diphenyl ethers (PBDE).^[24,36–44] Evidence is also emerging for inhibition by other polybrominated biphenyls (PBB), polychlorinated dibenzo-1,4-dioxins (PCDDs), polybrominated dibenzo-1,4-dioxins (PBDDs), and other PHAHs.^[45–48] For example, 2,3,7,8-tetrachlorodibenzodioxin (TCDD) decreased Dio activity in rats,^[49–51] the similarity of its topology to THs may contribute to its toxicity.^[52] Additionally, tetrabromobisphenol A (TBBPA) decreases T3 levels in zebrafish embryos and affects Dio expression.^[53,54]

Our analysis of intermolecular interactions such as XB is rooted in the terminology of Lewis acid/base theory – the donation of electron density from a Lewis base donor to a Lewis acid acceptor. In this context, we avoid the IUPAC terminology which assigns the XB acceptor as the Lewis base and the XB donor as the R–X* acceptor. The most widely discussed feature of XB is the concept of a σ -hole in the electrostatic potential (ESP) along the bond axis of a halogen atom.^[55] From the viewpoint of our group and others, this model, while observable, downplays the partial covalency of donor-acceptor interactions and limits the analysis of trends where discussion in terms of bonding theory is more intuitive.^[56–58] Further, the σ -hole observed in the electrostatic potential is a consequence of the occupation of MOs in the acceptor molecule.^[59] In C–X bonds, the composition of the bonding MO is weighted toward the electronegative X. As electronegativity decreases down the halogen group, the contribution of X to the bond decreases, specifically in the p-orbital aligned along the bond axis. As a result, electron density is depleted along the bond axis while the p-orbitals perpendicular to the axis are unaffected leaving a positive dimple in the electrostatic potential.^[59]

Within the bonding model, XB is described as the donation from a filled orbital on the Lewis base to an accepting R–X* orbital (Figure 1B).^[56,60–62] The decreased contribution of X to the R–X bonding orbital results in an increase in its contribution to the R–X* antibonding acceptor orbital as the X electronegativity decreases. The resulting large X lobe in R–X* can overlap more strongly with the filled donor MO for a more favorable XB interaction. The XB donor-acceptor interaction energy ($\Delta E_{d \rightarrow a}$), measuring the stabilization of the donor MO by donation into the acceptor MO, will be inversely related to the strength of the R–X bond. The weaker the bond, the lower the energy of the R–X* acceptor orbital. Because the bonds weaken down the halogen group, XB increases as $F < Cl < Br < I$. XB strengths are additionally dependent on the Lewis basicity of the donor (XB acceptor). Of the natural amino acids, Sec is the most nucleophilic, more so than the more abundant Cys, making it an ideal choice for deiodination.

Our group has previously explored the strengths of XB between PCBs, PBDEs, and THs and their possible inhibition of deiodinase activity.^[35,63,64] While various groups have investigated bonding within XB complexes using methods like Atoms-in-Molecules (AIM),^[65–68] we have focused on the Wiberg Bond Index as a cost-effective means to quantify trends in bond strength. This paper expands our examination to selected PCDDs, PBDDs, PBBs, and polybrominated benzene EDCs (Table 1). These molecules were selected from compounds reported to influence TH signaling and/or those listed on TEDX as potential EDCs. Trends in XB strengths were calculated using DFT from donor-acceptor complexes of the PHAHs with $MeSe^-$ as a simple model for the Sec active site. Interaction strengths depend on the halogen, its position, and the degree of substitution.

Table 1. PHAHs included in this study.

Class	PHAHs
	 <p>X = Cl, PCDD; = Br, PBDD PBB</p>
Monohalogenated dibenzo-1,4-dioxins	2-MC(B)DD
Dihalogenated dibenzo-1,4-dioxins	2,3-DC(B)DD, 2,7-DC(B)DD
Trihalogenated dibenzo-1,4-dioxins	2,3,7-TrC(B)DD, 2,3,7-TrC(B)DD
Tetrahalogenated dibenzo-1,4-dioxins	1,3,6,8-TC(B)DD, 1,3,7,9-TC(B)DD, 2,3,7,8-TC(B)DD
Pentahalogenated dibenzo-1,4-dioxins	1,2,3,7,8-PC(B)DD
Hexahalogenated dibenzo-1,4-dioxins	1,2,3,7,8,9-HC(B)DD, 1,2,3,4,7,8-HC(B)DD, 1,2,3,6,7,8-HC(B)DD
Heptahalogenated dibenzo-1,4-dioxin	1,2,3,4,6,7,8-HpC(B)DD (HpC(B)DD)
Octahalogenated dibenzo-1,4-dioxin	1,2,3,4,6,7,8,9-OC(B)DD (OC(B)DD)
Dibromobiphenyls	2,2'-PBB (PBB-4), 3,3'-PBB (PBB-11), 4,4'-PBB (PBB-15)
Tetrabromobiphenyls	2,2',4,4'-PBB (PBB-47), 2,2',6,6'-PBB (PBB-54), 3,3',4,4'-PBB (PBB-77)
Hexabromobiphenyls	2,2',4,4',5,5'-PBB (PBB-153), 2,2',4,4',6,6'-PBB (PBB-155), 3,3',-4,4',5,5'-PBB (PBB-169)
Heptabromobiphenyls	2,2',3,4,4',5,5'-PBB (PBB-180)
Decabromobiphenyl	DBB (PBB-207)
Polybrominated benzenes	2,4-dibromophenol, 2,4,6-tribromophenol, pentabromophenol (PBP), pentabromoethylbenzene (PBEB), tetrabromobisphenol A (TBBPA), decabromodiphenylethane (DBDPE)

Theoretical Methods

Structures of PHAHs and their complexes with MeSe^- were optimized with the M06-2X^[69] exchange-correlation functional using Gaussian09.^[70] This functional was found to perform well for the XB18 and XB51 test sets compared to CCSD(T) calculations.^[71] Slight shortening of the C–Cl bond in weak XB complexes is observed as previously reported. This effect could be attributed to reorganization of the R–X* orbital to increase the contribution of X which also affects the R–X bond by shifting the polarization toward the carbon end to shorten the bond.^[56,72] Carbon, hydrogen, and oxygen were represented with a triple- ζ basis set that included polarization functions. The Wadt-Hay effective core potential basis set was used for chlorine, bromine, and selenium and augmented with diffuse and polarization functions.^[73] Optimized geometries were confirmed as true minima by vibrational frequency analysis. Natural Bond Orbital (NBO) donor-acceptor interaction energies ($\Delta E_{d \rightarrow a}$) from second-order perturbation theory as the stabilization of a filled σ -type orbital by the interaction with an empty σ^* -type orbital, Wiberg bond indices (WBIs),^[74] and compositions of R–X orbitals were calculated values were calculated using NBO 3.0 as implemented in Gaussian 09.^[75] ESP and AIM calculations were performed using the Multiwfn package.^[76]

Results

XB strengths were calculated for the optimized complexes of MeSe^- with selected PCDDs, PBDDs, PBBs, and other potential EDCs (Table 1). Relative energies corrected for the zero-point vibrational energy for formation of the XB complex were calculated as $\Delta E_{\text{zpe}} = E_{\text{zpe}}(\text{XB complex}) - E_{\text{zpe}}(\text{PHAH}) - E_{\text{zpe}}(\text{MeSe}^-)$. In the following discussion, XB complexes are labeled according to the position at which XB takes place. For example, Se-2-OCDD indicates an XB interaction at the 2-position of OCDD.

Polyhalogenated Dibenzodioxins

Measures of XB strength ($\Delta E_{d \rightarrow a}$, WBIs, etc., Figure 2) are consistent with previously reported trends,^[56] with the stronger C–Cl bonds of PCDDs weakly interacting ($\Delta E_{\text{zpe}} = -2$ – -13 kcal/mol) with MeSe^- compared to the PBDDs ($\Delta E_{\text{zpe}} = -9$ – -26 kcal/mol). XB at the 1-position of OCDD and OBDD are the strongest of the series ($\Delta E_{\text{zpe}} = -12.1$ and -24.9 kcal/mol, respectively). Monohalogenated 2-PCDD forms the weakest XB interaction ($\Delta E_{\text{zpe}} = -2.0$ kcal/mol) with 2-PBDD (-10.2 kcal/mol) comparable to fully substituted OCDD. Increasing the substitution of electron withdrawing (EW) groups depletes the ring electron density and lowers the energy of the unoccupied ϕ_{R-X^*} orbitals (better Lewis acid) to strengthen the XB interaction (Figure 2A). Similar trends are found for the density at the XB critical point in AIM calculations (Figure 3), which is generally more than double for donation to the C–X bond of TBDD versus TCDD (Figure 3C). Ancillary hydrogen bonds to the MeSe^- methyl group can provide additional stabilization to the XB, especially for the weaker Cl \cdots Se interactions where the CH_3 protons are attracted to the chloride lone pairs (Figure 3C). As previously reported, the LUMOs of polychlorinated aromatics have π^* rather than C–Cl* character.^[56] In many of the PBDDs, the π^* MOs of the conjugated aromatic rings can also

be lower in energy than the C–Br* orbitals. The lowest C–Cl*-type orbitals of PCDDs are more destabilized relative to the HOMO compared to their PBDD analogues (Figure 4). These results are consistent with the relative strengths of the C–Cl and C–Br bonds.

The ΔE_{zpe} values for each set of PXDDs arrange into three clusters with respect to the %X contribution to the R–X* orbital (Figure 5). The weakest XBs are found for *meta* halogens with no adjacent EW group. PXDD with one EW group adjacent to a *meta* and *ortho* halogen increases the %X in R–X* and shifts to lower ΔE_{zpe} . Conversely, the decreasing %X contribution to the R–X bonding MO increases the size of the σ -hole in the ESP (Figure 5B). Having two adjacent EW groups further increases %X in the R–X* orbital for the most favorable overlap with the donor Se lp orbital and strongest series of XB interactions. Within each cluster, additional substitutions further increase the %X contribution for stronger XB interactions. In asymmetric PXDDs, interactions are stronger on the more substituted ring, but the inductive effect of substitutions on the other ring also influences XB strength. For example, in 1,2,3,4,7,8-HC(B)DD, the XB interaction on the disubstituted ring is 2–3 (6) kcal/mol lower in energy than tetrasubstituted ring and 1.3–1.4 kcal/mol lower than in 2,3,7,8-TC(B)DD.

The low contribution of Cl to the R–Cl* orbital (%Cl < 50%) limits its ability to overlap with the Se lp donor orbital compared to the less electronegative Br (%Br = 50–53%). Both halogens have lower %X contributions than R–I* orbitals which can exceed 60% in highly activated bonds.^[56] The donation of electron density into the R–X* orbital lengthens and activates the R–X bond and shortens the X \cdots Se distance in proportion to its bond strength (Figure 2B). The C–Cl bonds are least affected in PCDDs where increased chlorination contributes to activation by up to 0.025 Å with Cl \cdots Se close contacts ranging from 3.1 to 3.4 Å. In contrast, weaker C–Br bonds are lengthened by 0.04–0.25 Å with Br \cdots Se contacts ranging from 2.6 to 3.2 Å. The X \cdots Se bond distances correlate with the donor-acceptor energies ($\Delta E_{d \rightarrow a}$) with Cl \cdots Se values lower and covering a narrower range (4–14 kcal/mol) than for the PBDDs (18–61 kcal/mol) as expected from the relative C–X bond strengths. The shortest distances and strongest donor-acceptor interactions are found for the highly substituted OXDD (X=Cl, 3.12 Å, 13.8 kcal/mol (Se-1-OCDD); X=Br, 2.69 Å, 61.2 kcal/mol (Se-2-OBDD). At long X \cdots Se distances, the $\Delta E_{d \rightarrow a}$ values approach zero whereas at short distances the donor-acceptor interaction can exceed 60 kcal/mol. The short X \cdots Se distances are significantly less than the sum of the Se and X van der Waals distances (3.65 (Cl) and 3.75 (Br) Å) consistent with the partial covalent nature of XB interactions as described in the bonding model and measured by the accumulation of electron density in the X \cdots Se WBIs. In the strongest interactions, such as Se-2-OBDD, the Br \cdots Se WBI approaches 0.5, while the C–Br WBI decreases from 1.061 to 0.604, bond orders consistent with the three-center-four-electron (3c4e) hypervalent bond limit of a strong halogen bond.^[56,61,78,79] In contrast, Cl \cdots Se WBIs in PCDDs are lower than the weakest Br \cdots Se interactions with even the most highly substituted only 0.2.

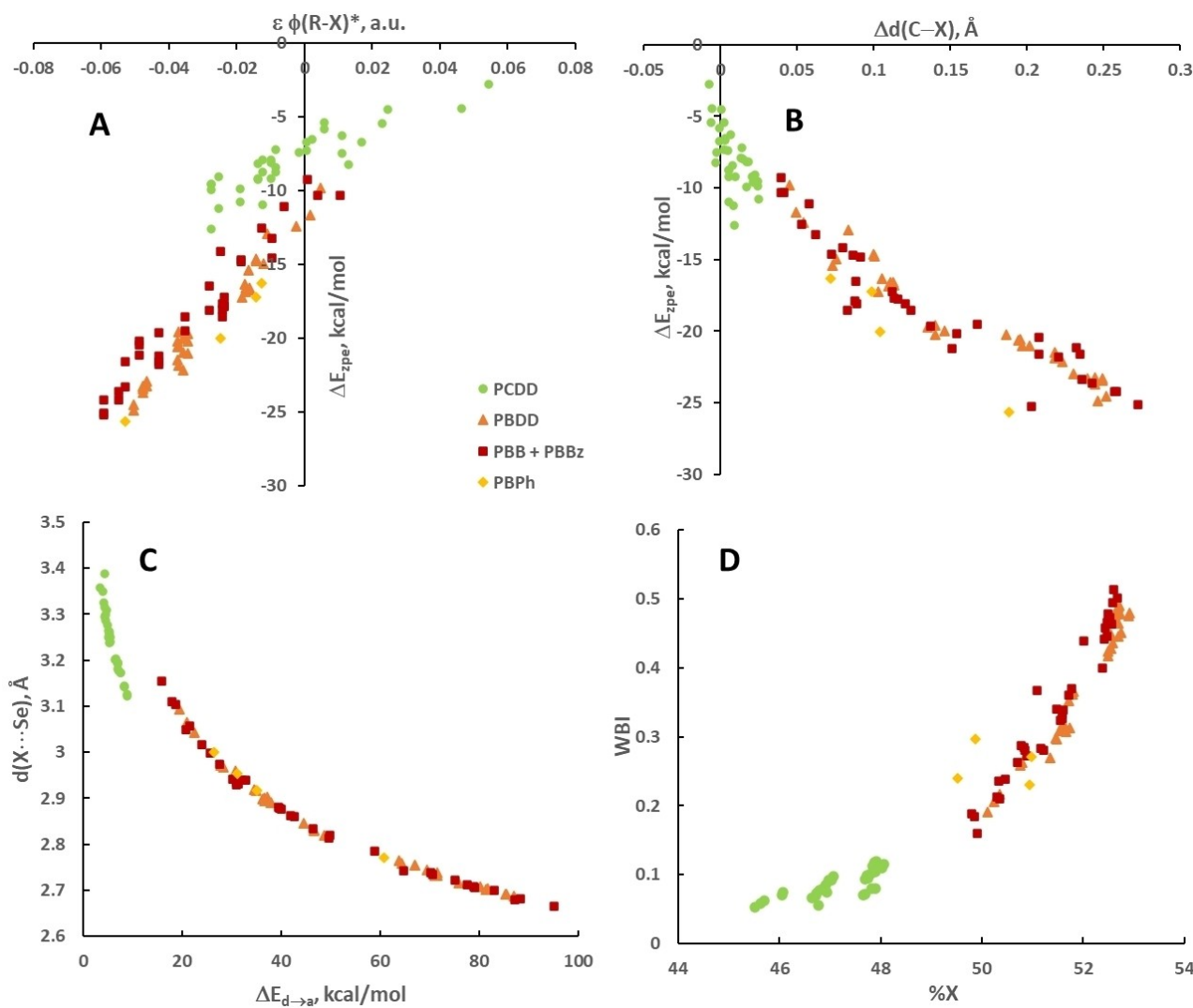


Figure 2. Relationships between (A) the R–X* orbital energy and the XB interaction energy, (B) the lengthening/activation of the C–X bond and the XB interaction energy, (C) the X⋯Se XB distance and the donor-acceptor energy, and (D) the %X contribution to the R–X* orbital for the set of PCDDs, PBDDs, PBB, polybrominated benzenes (PBBz) and polybrominated phenols (PBPh).

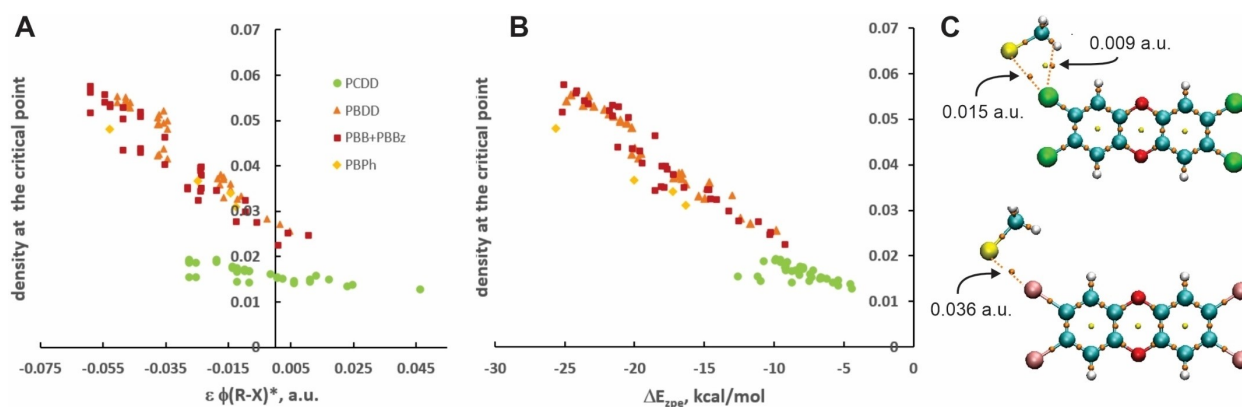


Figure 3. (A) Comparison of the electron density at the XB critical point from AIM calculations. The density increases with lower energy acceptor R–X* MOs. (B) Increased electron density at the XB critical point correlates with more favorable XB interactions. AIM calculations were performed using the Multiwfn software package. (C) QTAIM diagrams of the XB complexes of MeSe⁻ with 2,3,7,8-TCDD and 2,3,7,8-TBDD. Orange spheres and lines indicate critical points and connecting paths. Values for selected densities at the critical point ($\rho(r_c)$) are given.

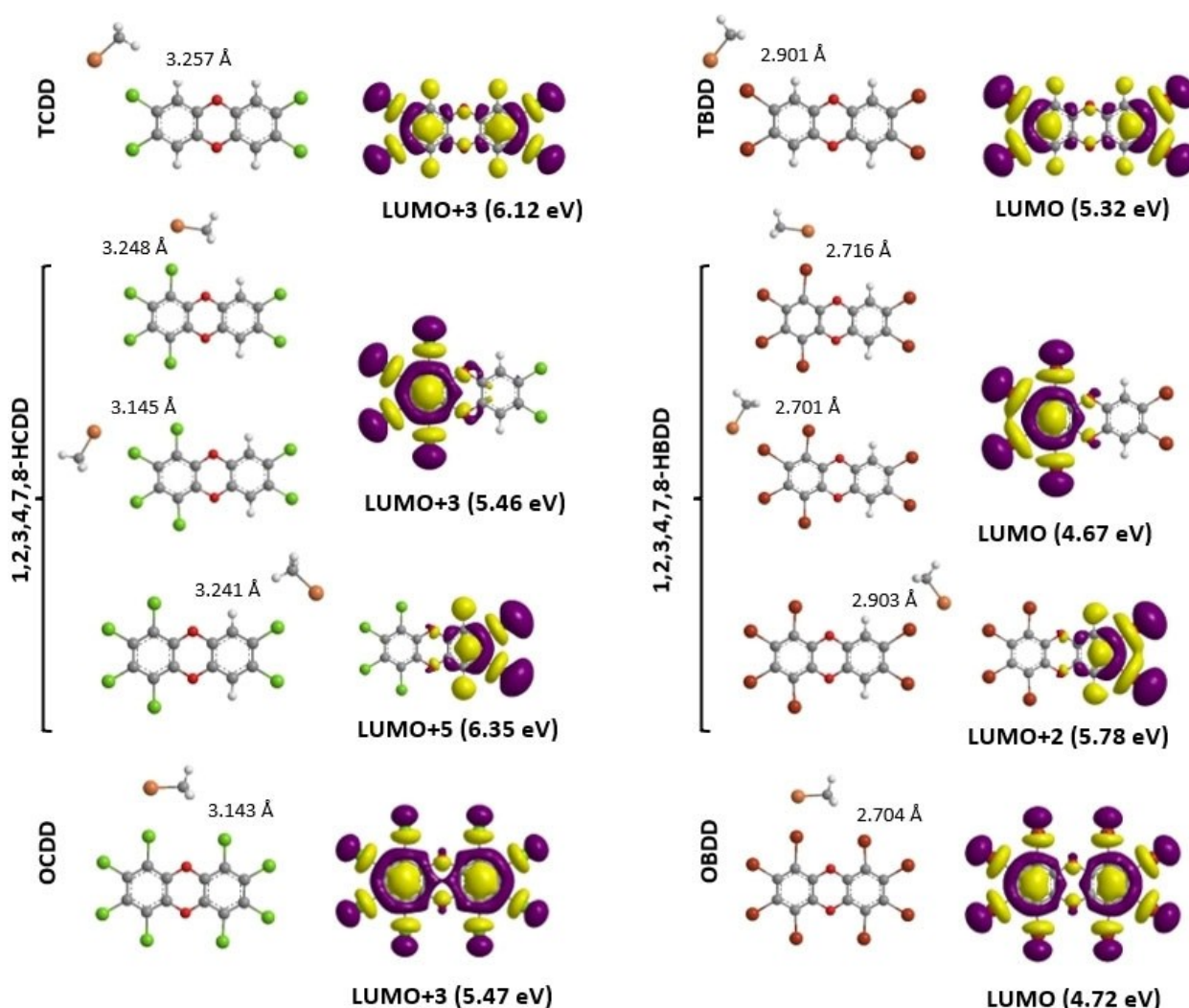


Figure 4. Selected optimized structures of PXDD-MeSe⁻ XB complexes with X...Se distances and corresponding R-X*-type orbitals. Energies of the LUMOs relative to the HOMO are provided in parentheses.

Polybrominated Benzenes and Biphenyls

XB complexes of a select series of eleven PBBs and six polybrominated benzenes/phenols were calculated for comparison to previous results for PCBs, PBDEs, and PBDDs (Figure 6). PBBs from stronger XB interactions than PCBs^[64] ($\Delta E_{zpe} = -2$ – -16 kcal/mol (PCBs) vs -9 – -26 kcal/mol (PBBs)) and generally follow similar trends to the PBDDs above for %Br contributions to the R-X* orbital and measures of XB strength ($\Delta E_{d\rightarrow a}$ WBIs, etc., Figure 2). For the disubstituted series 2,2'-PBB, 3,3'-PBB, and 4,4'-PBB, the *meta* and *para* positions with respect to the biphenyl bridge form similar XB interactions in terms of ΔE_{zpe} with $\Delta E_{d\rightarrow a}$ slightly more favorable for *meta*. As for PCBs, the strongest interactions overall in terms of ΔE_{zpe} are found at *ortho* positions flanked by additional bromine centers due to electrostatic interactions between the MeSe⁻ methyl group and the opposite ring. Donor-acceptor energies $\Delta E_{d\rightarrow a}$ tend to be most favorable at the *meta* and *para* positions. For example, the strongest interactions to 2,2',3,4,4',5,5'-PBB are to the 3-

and 4-positions ($\Delta E_{d\rightarrow a} = 75.1$ and 70.7 kcal/mol, respectively) of the most substituted ring. As for the PBDDs, the strong interactions of highly substituted PBBs have similarly activated C-Br bonds and Br...Se WBI bond orders close to 3c4e bonds (i.e., WBI=0.475 in Se-4-DBB and 0.461 in Se-4-DBDPE). The MeSe⁻ donor bridges the *ortho* bromines of the two rings of DBDPE with weaker individual XB interactions ($\Delta E_{d\rightarrow a} = 16.8$ kcal/mol), but a stronger than expected overall interaction ($\Delta E_{zpe} = -31.6$ kcal/mol).

Like PCBs, PBBs have been classified as coplanar (dioxin-like) or non-coplanar (non-dioxin-like) even though none of these molecules are coplanar. Early researchers made a false assumption about the dioxin-like potency of PCBs and PBBs lacking *ortho* substitutions, drawing these molecules as planar-like dioxins. For example, the potent 3,3',4,4',5,5'-PBB has a 41° dihedral angle between the rings. The high toxicity of the so-called coplanar or dioxin-like PBBs could be attributed to their greater flexibility for adapting to protein binding sites. The non-dioxin-like PBBs are locked into a twisted conformation

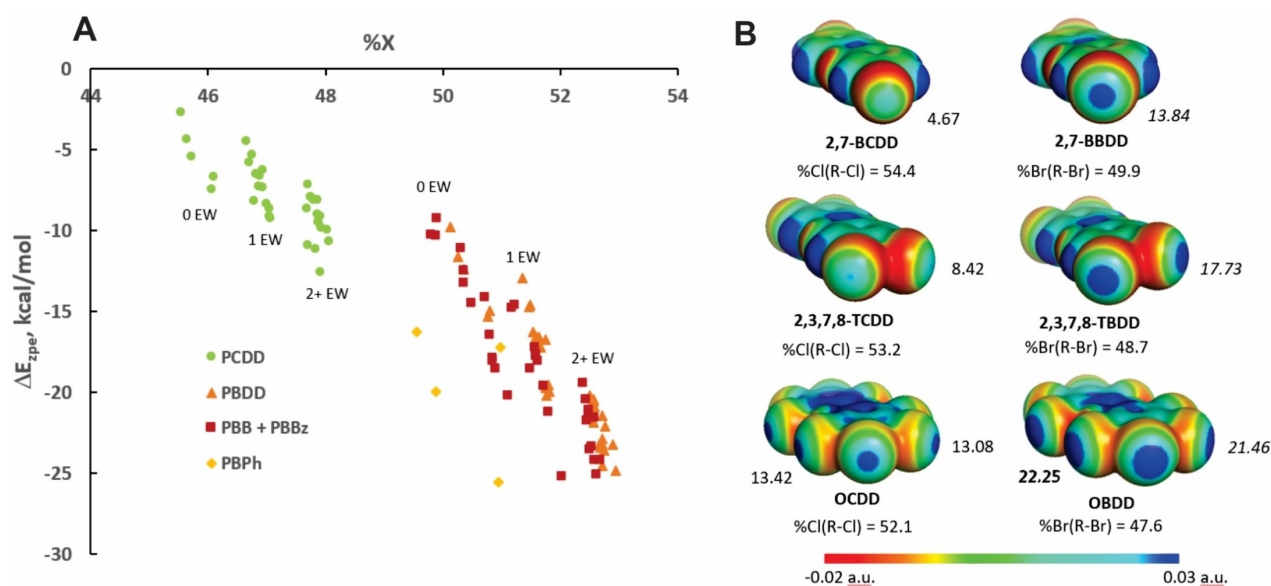


Figure 5. (A) Comparison of the XB interaction energy ΔE_{zpe} with the %X contribution to the R-X* orbital. Results cluster by the number of electron-withdrawing (EW) groups for the PCDDs, PBDDs, PBB, polybrominated benzenes (PBBz) and polybrominated phenols (PBPh). (B) ESP plots of selected PCDDs and PBDDs. Values of the potential at the σ -hole are given in kcal/mol. Note that the size of the σ -hole increases as the %X contribution to the R-X bonding MO decreases. Plots generated using PyMol.^[77]

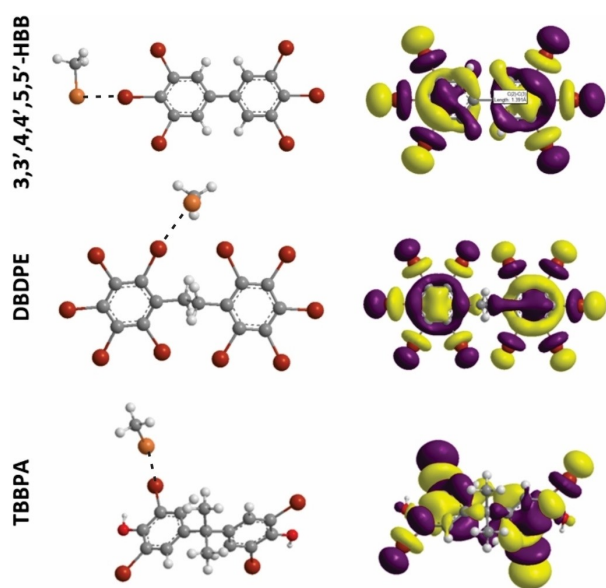


Figure 6. Selected optimized structures of polybrominated aromatic-MeSe⁻ XB complexes and corresponding R-Br*-type orbitals.

with the inter-ring dihedral angle near 90° with even less flexibility in the twist than PCBs due to the larger size of the bromine centers. While highly substituted PBBs like PBB-180 or PBB-207 may form strong interactions with MeSe⁻, their greater steric bulk and rigidity could limit their binding to Dio.

Polybrominated benzenes/phenols follow the same trends as other PHAHs with the exception that hydroxyl substitutions shift the trends for XB at positions *ortho* to hydroxyl groups (Figure 2). Of the series, the weakest interaction is found for Se-

4-2,4-DBP and the strongest for Se-2-PBP. Hydrogen bonding to Br draws electron density away from the Ips orthogonal to the XB axis for an overall stronger interaction. In Se-2-PBP, this electrostatic interaction stabilizes complex formation for Se-2-PBP (ΔE_{zpe}) over XB at the *meta* and *para* positions which have stronger donor-acceptor interactions (ΔE_{d-a} = 60.7 (*o*), 79.1 (*m*), 78.9 (*p*) kcal/mol). As a result, these examples, with the exception of TBBPA, are outliers to the general trends for polybrominated aromatics included in this study.

Discussion

Sufficient experimental data on Dio inhibition by these PHAHs is not yet available for comparisons with trends in XB strength. However, increase in XB strength would generally be expected to correlate with enhanced endocrine/thyroid disruption and Dio inhibition through tighter binding to the active site Sec. Nonetheless, the predictive power of these trends regarding regioselectivity is muted by the contributions of substrate interactions with the residues of the binding pocket. The strongest interactions to T₄ are found for the outer ring iodines, which, while consistent with the selectivity of Dio2, inner ring deiodination by Dio3 demonstrates that the manner of TH binding to the active site contributes significantly to selectivity. However, the trends in XB strength may provide insight into the potential for a PHAH to undergo dehalogenation or reversibly bind to the active site. From the lack of deiodination of 3-T₁ at the low end of the TH range, we proposed a threshold for the initial XB interaction that needs to be exceeded for dehalogenation to take place.^[35] The range of XB strengths for polybrominated aromatics overlap with that expected for iodothyronines (ΔE_{zpe} = -21--33 kcal/mol) with

at least one position of several highly substituted polybrominated aromatics similar to that of 3-T₁ (e.g., Se-4-HpBDD (−23.7 kcal/mol), Se-1-OBDD (−24.9 kcal/mol), Se-2-PBB-207 (−25.2 kcal/mol), and Se-1-PBP (−25.6 kcal/mol)) suggesting the potential for debromination of these molecules. Highly substituted PBDEs that XB to MeSe[−] with similar strength to THs have been shown to be debrominated by Dio proteins.^[80,81] However, PCDDs are substantially weaker, even for the most substituted congeners, and would not be expected to undergo dehalogenation by Dios, nor have these products been observed experimentally.

Full bond breaking in the gas phase is limited by the instability of the aromatic carbanion but is facilitated by protonation in the protein or bulk solvent. The insignificant activation of the C–Cl bond (or the C–Br bond in low substitution brominated aromatics) does not allow for enough negative charge to accumulate on carbon for it to have sufficient proton affinity to undergo dehalogenation. Trapping the Dio active site through XB of a nonreactive PHAH inhibits activity by blocking TH binding and deiodination. In the case of Dio2, which turns over more slowly than Dio1 and Dio3, PHAH binding or debromination may cause ubiquitination and destruction of the protein.

Just as Dio reacts regioselectively with THs, PHAHs may be most effective against Dios with similar substitutions.^[35] Where Dio1 deiodinates at either site and may be inhibited by a wide range of PHAHs, Dio2 activates T4 to T3 by removing an outer-ring iodine, which is *meta* to the ether linkage to the inner ring. The similarity between TBBPA and the outer ring of T4 gives it high affinity for transthyretin,^[82] suggesting that it may also affect Dio2, likely through an unreactive XB interaction given the magnitude of its XB interaction ($\Delta E_{zpe} = -13.3$ kcal/mol). PHAHs capable of XB at the *meta* position, such as 2,3,7,8-TC(B)DD and 3,3',4,4',5,5'-PBB, may be more effective against this Dio and maintain low conversion to T3. For the highly potent 2,3,7,8-PCDD, the four-fold symmetry of dioxin centers with *meta* halogens may be similar enough to the topology of thyroxine's outer ring to strongly interact with TH binding sites such as in Dio2. Increasing the degree of halogen substitution could strengthen the interaction, for example Se-2-HCDD is slightly stronger than Se-2-TCDD ($\Delta E_{zpe} = -9.2$ vs -6.6 , respectively). Dio3 deactivates T3 and T4 by removing an inner-ring iodine, which is *ortho* to the linkage to the outer ring. PHAHs with favorable XB at the *ortho* position, such as OC(B)DD or 2,2',4,4'-PBB, may preferentially inhibit Dio3. In either case, considering the XB interaction strength alone using the simple MeSe[−] model is insufficient to predict binding trends for the protein because secondary interactions with the binding pocket are omitted. For example, an O...I interaction detected in molecular dynamics simulations may contribute to the regioselectivity of Dio3 for inner-ring deiodination.^[9]

Conclusions

Polyhalogenated organic compounds are well known to disrupt endocrine signaling processes. In addition to the major pathway of binding to AhR, these PHAHs may also inhibit the

thyroid hormone activating/deactivating Dio proteins through XB to the active site Sec. Interactions of the PCDD, PBDD, and PBB classes of potential EDCs with MeSe[−] as a simple model of the Dio active site Sec follow the expected trends for XB (Br > Cl). Donation into the weaker C–Br bonds is facilitated by low-lying C–Br* orbitals that are weighed toward the halogen for stronger overlap with the donor orbital. XB strengths are additionally dependent on the position of the halogen and the degree of substitution. Halogens *meta* to the dioxin bridge or the biphenyl linkage are preferred. Adjacent electron withdrawing groups also activate the C–X bonds for stronger XB interactions. Although these calculations shed light on XB trends in these PHAHs, they are less effective for predicting inhibition of Dio in the absence of knowledge of the interactions with the Dio active site. PHAHs that are topologically similar to target THs are expected to have the highest affinity for Dios, transport, and receptor proteins. Future experimental work on the relationship between PHAH exposure and Dio activity would help to clarify the role of XB and provide knowledge of topography of the TH binding site that may aid in drug design.

Acknowledgements

Calculations were performed on the Turing High Performance Cluster maintained by ODU Information Technology Services.

Conflict of Interests

The authors declare no conflict of interest.

Data Availability Statement

The data that support the findings of this study are available from the corresponding author upon reasonable request.

Keywords: Halogen bonding · Density functional theory · Endocrine disrupting compounds · Thyroid hormones · Molecular Orbital Theory

- [1] G. Cavallo, P. Metrangolo, R. Milani, T. Pilati, A. Priimagi, G. Resnati, G. Terraneo, *Chem. Rev.* **2016**, *116*, 2478–2601.
- [2] P. R. Varadwaj, A. Varadwaj, H. M. Marques, *Inorganics* **2019**, *7*, 40.
- [3] C. A. Bayse, E. R. Rafferty, *Inorg. Chem.* **2010**, *49*, 5365–5367.
- [4] J. Köhrle, in *Methods in Enzymology* (Eds.: H. Sies, L. Packer), Academic Press, **2002**, pp. 125–167.
- [5] A. C. Bianco, D. Salvatore, B. Gereben, M. J. Berry, P. R. Larsen, *Endocr. Rev.* **2002**, *23*, 38–89.
- [6] A. C. Bianco, B. W. Kim, *J. Clin. Invest.* **2006**, *116*, 2571–2579.
- [7] D. Manna, G. Mugesh, *Angew. Chem. Int. Ed.* **2010**, *122*, 9432–9435.
- [8] D. Manna, G. Mugesh, *J. Am. Chem. Soc.* **2012**, *134*, 4269–4279.
- [9] C. A. Bayse, E. S. Marsan, J. R. Garcia, A. T. Tran-Thompson, *Sci. Rep.* **2020**, *10*, 15401.
- [10] D. Cesario, M. Fortino, T. Marino, F. Nunzi, N. Russo, E. Sicilia, *J. Comput. Chem.* **2019**, *40*, 944–951.
- [11] K. Arai, H. Toba, N. Yamamoto, M. Ito, R. Mikami, *Chem. Eur. J.* **2023**, *29*, e202202387, <https://doi.org/10.1002/chem.202202387>.
- [12] U. Schweizer, C. Schlicker, D. Braun, J. Köhrle, C. Steegborn, *Proc. Natl. Acad. Sci. USA* **2014**, *111*, 10526–10531.

- [13] "TEDX – The Endocrine Disruption Exchange," can be found under <https://endocrinedisruption.org/home/>, n.d.
- [14] G. Mason, K. Farrell, B. Keys, J. Piskorska-Pliszczynska, L. Safe, S. Safe, *Toxicology* **1986**, *41*, 21–31.
- [15] G. Mason, T. Zacharewski, M. A. Denomme, L. Safe, S. Safe, *Toxicology* **1987**, *44*, 245–255.
- [16] M. W. Hornung, E. W. Zabel, R. E. Peterson, *Toxicol. Appl. Pharmacol.* **1996**, *140*, 227–234.
- [17] T. Hamers, J. H. Kamstra, E. Sonneveld, A. J. Murk, M. H. A. Kester, P. L. Andersson, J. Legler, A. Brouwer, *Toxicol. Sci.* **2006**, *92*, 157–173.
- [18] P. A. Behnisch, K. Hosoe, S. Sakai, *Environ. Int.* **2003**, *29*, 861–877.
- [19] K. J. Oliveira, M. I. Chiamolera, G. Giannocco, C. C. Pazos-Moura, T. M. Ortiga-Carvalho, *J. Mol. Endocrinol.* **2019**, *62*, R1–R19.
- [20] A. Brouwer, D. C. Morse, M. C. Lans, A. G. Schuur, A. J. Murk, E. Klasson-Wehler, A. Bergman, T. J. Visser, *Toxicol. Ind. Health* **1998**, *14*, 59–84.
- [21] C. E. Francis, L. Allee, H. Nguyen, R. D. Grindstaff, C. N. Miller, S. Rayalam, *Toxicology* **2021**, *463*, 152972.
- [22] V. Dichiarante, G. Cavallo, P. Metrangolo, *Current Op. Green Sustainable Chem.* **2021**, *30*, 100485.
- [23] B. B. Mughal, J.-B. Fini, B. A. Demeneix, *Endocrine Conn.* **2018**, *7*, R160–R186.
- [24] S. D. Soechitram, S. A. Berghuis, T. J. Visser, P. J. J. Sauer, *Sci. Total Environ.* **2017**, *574*, 1117–1124.
- [25] M. G. Wade, S. Parent, K. W. Finnson, W. Foster, E. Younglai, A. McMahon, D. G. Cyr, C. Hughes, *Toxicol. Sci.* **2002**, *67*, 207–218.
- [26] X.-M. Ren, L.-H. Guo, *Environ. Sci. Process. Impacts* **2013**, *15*, 702–708.
- [27] R. T. Zoeller, *Mol. Cell. Endocrinol.* **2005**, *242*, 10–15.
- [28] A.-K. Mortensen, J. Verreault, A. Francois, M. Houde, M. Giraud, M. Dam, B. M. Jessen, *Sci. Total Environ.* **2022**, *806*, 150506.
- [29] M. Alae, P. Arias, A. Sjodin, A. Bergman, *Environ. Int.* **2003**, *29*, 683–689.
- [30] J. L. Lyche, C. Rosseland, G. Berge, A. Polder, *Environ. Int.* **2015**, *74*, 170–180.
- [31] H. a. N. GuanGen, D. GangQiang, L. O. U. XiaoMing, W. XiaoFeng, H. a. N. JianLong, S. HaiTao, Z. Yu, D. U. LeYan, *Biomed. Environ. Sci.* **2011**, *24*, 112–116.
- [32] L.-C. Guo, S. Yu, D. Wu, J. Huang, T. Liu, J. Xiao, W. Huang, Y. Gao, X. Li, W. Zeng, S. Rutherford, W. Ma, Y. Zhang, L. Lin, *Environ. Pollut.* **2019**, *254*, 112925.
- [33] V. Singh, J. Cortes-Ramirez, L.-M. Toms, T. Sooriyagoda, S. Karatela, *Intern. J. Environ. Res. Pub. Health* **2022**, *19*, 7820.
- [34] K. W. Bock, C. Köhle, *Biochem. Pharmacol.* **2006**, *72*, 393–404.
- [35] E. S. Marsan, C. A. Bayse, *Molecules* **2020**, *25*, 1328.
- [36] C. M. Butt, D. Wang, H. M. Stapleton, *Toxicol. Sci.* **2011**, *124*, 339–347.
- [37] S. Llop, M. Murcia, M. Alvarez-Pedrerol, J. O. Grimalt, L. Santa-Marina, J. Julvez, F. Goñi-Irigoyen, M. Espada, F. Ballester, M. Rebagliato, M.-J. Lopez-Espinosa, *Environ. Int.* **2017**, *104*, 83–90.
- [38] S. C. Roberts, A. C. Bianco, H. M. Stapleton, *Chem. Res. Toxicol.* **2015**, *28*, 1265–1274.
- [39] P. D. Noyes, D. E. Hinton, H. M. Stapleton, *Toxicol. Sci.* **2011**, *122*, 265–274.
- [40] V. Beck, S. A. Roelens, V. M. Darras, *Gen. Comp. Endocrinol.* **2006**, *148*, 327–335.
- [41] M. Couderc, J. Marchand, A. Zalouk-Vergnoux, A. Kamari, B. Moreau, I. Blanchet-Letrouye, B. Le Bizec, C. Mouneyrac, L. Poirier, *Sci. Total Environ.* **2016**, *550*, 391–405.
- [42] S. Jarque, B. Piña, *Environ. Res.* **2014**, *135*, 361–375.
- [43] D. C. Morse, E. K. Wehler, W. Wesseling, J. H. Koeman, A. Brouwer, *Toxicol. Appl. Pharmacol.* **1996**, *136*, 269–279.
- [44] U. Schweizer, H. Towell, A. Vit, A. Rodriguez-Ruiz, C. Steegborn, *Mol. Cell. Endocrinol.* **2017**, *458*, 57–67.
- [45] X. Wang, S. Ling, K. Guan, X. Luo, L. Chen, J. Han, W. Zhang, B. Mai, B. Zhou, *Environ. Sci. Technol.* **2019**, *53*, 8437–8446.
- [46] T. A. Smythe, C. M. Butt, H. M. Stapleton, K. Pleskach, G. Ratnayake, C. Y. Song, N. Riddell, A. Konstantinov, G. T. Tomy, *Environ. Sci. Technol.* **2017**, *51*, 7245–7253.
- [47] D. Lee, C. Ahn, E.-J. Hong, B.-S. An, S.-H. Hyun, K.-C. Choi, E.-B. Jeung, *Int. J. Environ. Res. Public Health* **2016**, *13*, 697.
- [48] L. S. Birnbaum, D. F. Staskal, J. J. Diliberto, *Environ. Int.* **2003**, *29*, 855–860.
- [49] S. Eltom, J. Babish, D. Ferguson, *Toxicol. Lett.* **1992**, *61*, 125–139.
- [50] A. Raasmaja, M. Viluksela, K. K. Rozman, *Toxicology* **1996**, *114*, 199–205.
- [51] M. Viluksela, A. Raasmaja, M. Lebofsky, B. U. Stahl, K. K. Rozman, *Toxicol. Lett.* **2004**, *147*, 133–142.
- [52] M. Pavuk, A. J. Schecter, F. Z. Akhtar, J. E. Michalek, *Ann. Epidemiol.* **2003**, *13*, 335–343.
- [53] Y. Yu, Y. Hou, Y. Dang, X. Zhu, Z. Li, H. Chen, M. Xiang, Z. Li, G. Hu, *J. Hazard. Mater.* **2021**, *414*, 125408.
- [54] A. Parsons, A. Lange, T. H. Hutchinson, S. Miyagawa, T. Iguchi, T. Kudoh, C. R. Tyler, *Aquat. Toxicol.* **2019**, *209*, 99–112.
- [55] P. Politzer, P. Lane, M. Concha, Y. Ma, J. Murray, *J. Mol. Model.* **2007**, *13*, 305–311.
- [56] C. A. Bayse, *New J. Chem.* **2018**, *42*, 10623–10632.
- [57] V. Angarov, S. Kozuch, *New J. Chem.* **2018**, *42*, 1413–1422.
- [58] M. Palusiak, *J. Mol. Struct.* **2010**, *945*, 89–92.
- [59] T. Clark, M. Hennemann, J. Murray, P. Politzer, *J. Mol. Model.* **2007**, *13*, 291–296.
- [60] G. Manca, A. Ienco, C. Mealli, *Cryst. Growth Des.* **2012**, *12*, 1762–1771.
- [61] G. C. Pimentel, *J. Chem. Phys.* **1951**, *19*, 446–448.
- [62] M. Tawfik, K. J. Donald, *J. Phys. Chem. A* **2014**, *118*, 10090–10100.
- [63] E. S. Marsan, C. A. Bayse, *Chem. Eur. J.* **2017**, *23*, 6625–6633.
- [64] E. S. Marsan, C. A. Bayse, *Chem. Eur. J.* **2020**, *26*, 5200–5207.
- [65] J.-W. Zou, Y.-X. Lu, Q.-S. Yu, H.-X. Zhang, Y.-J. Jiang, *Chin. J. Chem.* **2006**, *24*, 1709–1715.
- [66] N. J. Martinez Amezaga, S. C. Pamies, N. M. Peruchena, G. L. Sosa, *J. Phys. Chem. A* **2010**, *114*, 552–562.
- [67] D. J. R. Duarte, G. L. Sosa, N. M. Peruchena, *J. Mol. Model.* **2013**, *19*, 2035–2041.
- [68] M. L. Kuznetsov, *Int. J. Quantum Chem.* **2019**, *119*, e25869.
- [69] Y. Zhao, D. G. Truhlar, *Theor. Chem. Acc.* **2008**, *120*, 215–241.
- [70] M. J. Frisch, G. W. Trucks, H. B. Schlegel, G. E. Scuseria, M. A. Robb, J. R. Cheeseman, G. Scalmani, V. Barone, B. Mennucci, G. A. Petersson, H. Nakatsuji, M. Caricato, X. Li, H. P. Hratchian, A. F. Izmaylov, J. Bloino, G. Zheng, J. L. Sonnenberg, M. Hada, M. Ehara, K. Toyota, R. Fukuda, J. Hasegawa, M. Ishida, T. Nakajima, Y. Honda, O. Kitao, H. Nakai, T. Vreven, J. A. Montgomery Jr., J. E. Peralta, F. Ogliaro, M. Bearpark, J. J. Heyd, E. Brothers, K. N. Kudin, V. N. Staroverov, R. Kobayashi, J. Normand, K. Raghavachari, A. Rendell, J. C. Burant, S. S. Iyengar, J. Tomasi, M. Cossi, N. Rega, J. M. Millam, M. Klene, J. E. Knox, J. B. Cross, V. Bakken, C. Adamo, J. Jaramillo, R. Gomperts, R. E. Stratmann, O. Yazyev, A. J. Austin, R. Cammi, C. Pomelli, J. W. Ochterski, R. L. Martin, K. Morokuma, V. G. Zakrzewski, G. A. Voth, P. Salvador, J. J. Dannenberg, S. Dapprich, A. D. Daniels, Ö. Farkas, J. B. Foresman, J. V. Ortiz, J. Cioslowski, D. J. Fox, Gaussian 09, Gaussian, Inc., Wallingford CT, **2009**.
- [71] S. Kozuch, J. M. L. Martin, *J. Chem. Theory Comput.* **2013**, *9*, 1918–1931.
- [72] S. J. Grabowski, *J. Phys. Chem. A* **2011**, *115*, 12340–12347.
- [73] W. R. Wadt, P. J. Hay, *J. Chem. Phys.* **1985**, *82*, 284–298.
- [74] K. B. Wiberg, *Tetrahedron* **1968**, *24*, 1083–1096.
- [75] P. Metrangolo, G. Resnati, *Chem. Eur. J.* **2001**, *7*, 2511–2519.
- [76] T. Lu, F. Chen, *J. Comput. Chem.* **2012**, *33*, 580–592.
- [77] PyMol, version 2.0, Schrödinger, Inc., **2015**.
- [78] R. J. Hach, R. E. Rundle, *J. Am. Chem. Soc.* **1951**, *73*, 4321–4324.
- [79] D. Li, T. Xia, W. Feng, L. Cheng, *RSC Adv.* **2021**, *11*, 32852–32860.
- [80] A. François, R. Técher, M. Houde, P. Spear, J. Verreault, *Environ. Toxicol. Chem.* **2016**, *35*, 2215–2222.
- [81] Y.-L. Luo, X.-J. Luo, M.-X. Ye, L. Lin, Y.-H. Zeng, B.-X. Mai, *Environ. Pollut.* **2019**, *246*, 710–716.
- [82] I. Meerts, J. J. van Zanden, E. a. C. Luijckx, I. van Leeuwen-Bol, G. Marsh, E. Jakobsson, A. Bergman, A. Brouwer, *Toxicol. Sci.* **2000**, *56*, 95–104.

Submitted: March 1, 2023

Accepted: May 4, 2023